[CANCER RESEARCH 59, 128–134, January 1, 1999]

# Chemical Design of Radiolabeled Antibody Fragments for Low Renal Radioactivity Levels[1]

**Yasushi Arano,[2] Yasushi Fujioka, Hiromichi Akizawa, Masahiro Ono, Tomoya Uehara, Kouji Wakisaka, Morio Nakayama, Harumi Sakahara, Junji Konishi, and Hideo Saji**

*Department of Patho-Functional Bioanalysis, Graduate School of Pharmaceutical Sciences [Y. A., Y. F., H. A., M. O., T. U., K. W., H. Saj.], and Department of Nuclear Medicine and Diagnostic Imaging, Graduate School of Medicine [H. Sak., J. K.], Kyoto University, Kyoto 606-8501; and Faculty of Pharmaceutical Sciences, Kumamoto University, Kumamoto 862-0973 [M. N.], Japan*

## ABSTRACT

**The renal uptake of radiolabeled antibody fragments presents a problem in targeted imaging and therapy. We hypothesized that the renal radioactivity levels of radiolabeled antibody fragments could be reduced if radiolabeled compounds of urinary excretion were released from glomerularly filtered antibody fragments before they were incorporated into renal cells by the action of brush border enzymes, present on the lumen of renal tubules. 3′-[$^{131}$I]Iodohippuryl $N^{\epsilon}$-maleoyl-L-lysine ([$^{131}$I]HML) was conjugated with a thiolated Fab fragment because the glycyl-lysine sequence in HML is a substrate for a brush border enzyme and *meta*-iodohippuric acid is released by cleavage of the linkage. Fab fragments were also radiolabeled by direct radioiodination ($^{125}$I-Fab) or by conjugation with *meta*-[$^{125}$I]-iodohippuric acid *via* an amide bond [*N*-(5-maleimidopentyl) 3′-iodohippuric acid amide ([$^{125}$I]MPH-Fab)] or an ester bond [maleimidoethy 3′-iodohippurate ([$^{125}$I]MIH-Fab)] by procedures similar to those used for [$^{131}$I]HML-Fab.**

**In biodistribution experiments in mice, [$^{131}$I]HML-Fab demonstrated markedly low renal radioactivity levels with kidney:blood ratios of radioactivity of 1 from 10 min to 1 h due to rapid release of *meta*-[$^{131}$I]iodohippuric acid. [$^{125}$I]MIH-Fab and $^{125}$I-Fab reached their peak ratios of 3.8 and 7.3 at 1 h, respectively, and [$^{125}$I]MPH-Fab showed the maximum ratio of 16.8 at 6 h. In subcellular distribution studies, both [$^{125}$I]MIH-Fab and $^{125}$I-Fab showed migration of radioactivity from the membrane to the lysosomal fraction of the renal cells from 10 to 30 min postinjection, whereas the majority of the radioactivity was detected only in the membrane fraction after administration of [$^{131}$I]HML-Fab at both time points. In nude mice, [$^{131}$I]HML-Fab showed one-quarter of the renal radioactivity of simultaneously administered $^{125}$I-Fab without impairing the target radioactivity levels 3 h after injection. These findings indicated that HML is a useful reagent for targeted imaging and therapy using antibody fragments as vehicles. These findings also suggested that the radiochemical design of radiolabeled antibody fragments that liberate radiometabolites of urinary excretion from antibody fragments by the action of brush border enzymes may constitute a new strategy for reducing the renal radioactivity levels of antibody fragments.**

## INTRODUCTION

LMW[3] antibody fragments such as Fab and single-chain Fv fragments provide rapid tumor targeting and uniform distribution in tumor tissues (1). Such characteristics render antibody fragments attractive vehicles for the delivery of radioactivity to tumor tissues for both targeted imaging and radiotherapy. However, high and persistent localization of the radioactivity is observed in the kidneys, which compromises tumor visualization in the kidney region and limits therapeutic potential (2–5). Indeed, $^{67}$Ga-labeled Fv fragments indicated a specific:nonspecific tumor ratio of radioactivity of 6 at 90 min postinjection, whereas the renal radioactivity levels reached 205% ID/g of tissue at the same postinjection time (6). Thus, radiolabeled LMW antibody fragments would become much more useful for targeted imaging and targeted therapy if the renal radioactivity levels could be reduced without impairing those in the target tissues.

Previous studies indicated that radiolabeled antibody fragments are most likely reabsorbed by proximal tubules *via* luminal endocytosis after glomerular filtration (7–13). The long residence times of the radiometabolites generated after lysosomal proteolysis of radiolabeled antibody fragments in renal cells were also reported to be responsible for the persistent renal radioactivity levels (5, 6, 14–16).

Two major strategies have been developed to reduce the renal radioactivity levels of radiolabeled antibody fragments. One is the blocking of reabsorption of radiolabeled antibody fragments themselves into renal cells by infusion of basic amino acids such as L-lysine so that the radiolabeled antibody fragments appear directly in the urine without being incorporated and metabolized in lysosomes of renal proximal cells. The other strategy involves interposition of a cleavable linkage between an antibody fragment and a radiolabeled compound of urinary excretion so that the radiolabeled compound is excreted from the lysosomal compartments of renal cells into the urine after lysosomal proteolysis of the radiolabeled antibody fragment in renal cells. Previous studies of renal handling of radiolabeled antibody fragments support the rationale of the two approaches. Indeed, successful reduction of renal radioactivity levels was demonstrated by the former approach using Fab and Fv fragments (17–19). However, further studies of administration dose and timing of basic amino acids as well as the toxicity of amino acids given in high doses will be required before the former approach can be used routinely (19, 20). Although the latter approach was extensively investigated and shown to reduce the hepatic radioactivity levels of intact antibodies, there have been only a few studies of LMW antibody fragments (21–23), and further studies may be required with regard to the relationship between chemical structures of radiometabolites and their elimination rates from the lysosomal compartments of renal cells. In addition, a previous study showed that use of ester bonds as the cleavable linkage may impair the target radioactivity levels delivered by antibody fragments due to cleavage of the ester bonds while the radiolabeled antibody fragments are circulating in plasma (23).

Meanwhile, studies of renal handling of LMW peptides indicated that some glomerularly filtered peptides are hydrolyzed to free amino acids during a short contact time with the brush border enzymes present on the lumen of the renal proximal cells (11). Indeed, several peptidases have been identified on the brush border membrane of renal tubules (24). These findings suggested that the renal localization of radioactivity may be reduced if radiolabeled compounds of urinary

Received 7/3/98; accepted 10/29/98.

The costs of publication of this article were defrayed in part by the payment of page charges. This article must therefore be hereby marked *advertisement* in accordance with 18 U.S.C. Section 1734 solely to indicate this fact.

[1] This work was supported in part by Grants-in-Aid (08557135 and 09672279) from the Ministry of Education, Science, Sports and Culture of Japan (both to Y. A.).

[2] To whom requests for reprints should be addressed, at Department of Patho-Functional Bioanalysis, Graduate School of Pharmaceutical Sciences, Kyoto University, Sakyo-ku, Kyoto 606-8501, Japan. Phone: 81-75-753-4608; Fax: 81-75-753-4568; E-mail: arano@pharm.kyoto-u.ac.jp.

[3] The abbreviations used are: LMW, low molecular weight; % ID, percentage injected dose; HML, 3′-iodohippuryl $N^{\epsilon}$-maleoyl-L-lysine; mAb, monoclonal antibody; 2-IT, 2-iminothiolane; MPH, *N*-(5-maleimidopentyl) 3′-iodohippuric acid amide; MIH, maleimidoethy 3′-iodohippurate; SHML, 3′-(tri-*n*-butylstannyl)hippuryl $N^{\epsilon}$-maleoyl-L-lysine; SMPH, *N*-(5-maleimidopentyl) 3′-(tri-*n*-butylstannyl)hippuric acid amide; SMIH, maleimidoethy 3′-(tri-*n*-butylstannyl)hippurate; HPLC, high-performance liquid chromatography; RP-HPLC, reversed-phase HPLC; PB, phosphate buffer; NCS, *N*-chlorosuccinimide; BB, borate buffer.



Downloaded from http://aacrjournals.org/cancerres/article-pdf/59/1/128/3228790/ch0199900128o.pdf by guest on 05 November 2024

excretion are liberated from the antibody fragments before they are incorporated into the renal cells by the action of the brush border enzymes. This strategy may be advantageous in reducing the renal radioactivity levels at early postinjection times because radiolabeled compounds are released from antibody fragments before they are incorporated and transported to the lysosomal compartment of the renal cells. This approach may be applicable to antibody fragments that are internalized into target cells if radiolabeled compounds released from the protein molecules at the renal tubules are excreted rapidly into urine but are retained within the target cells for long postinjection intervals.

To verify this hypothesis, *meta*-iodohippuric acid was selected as the radiolabeled compound because of its rapid urinary excretion from the renal tubular lumen and high stability against *in vivo* deiodination (25, 26). Because the glycyl-lysine sequence is a substrate for one of the brush border enzymes, carboxypeptidase M (27), present on the lumen of renal tubules, [$^{131}$I]HML was conjugated to the Fab fragment of a mAb against osteogenic sarcoma after treatment of the antibody fragment with 2-IT. When the peptide bond between the glycine and the lysine in HML is cleaved, *meta*-iodohippuric acid is released from the conjugate. The tissue distribution and subcellular distribution of the radioactivity after administration of [$^{131}$I]HML-Fab were compared to those of simultaneously administered $^{125}$I-Fab prepared by direct radioiodination of Fab fragment. In addition, *meta*-[$^{125}$I]iodohippuric acid was also conjugated to Fab fragments *via* an ester bond ([$^{125}$I]MIH-Fab) or an amide bond ([$^{125}$I]MPH-Fab) by procedures similar to those used for [$^{131}$I]HML-Fab. Previous studies indicated that, although MIH-conjugated polypeptides generated *meta*-iodohippuric acid as the sole radiometabolite after lysosomal proteolysis in hepatocytes, the radiometabolites derived from MPH-conjugated polypeptide showed long residence times in hepatocytes (23, 25, 26, 28). The chemical structures of the radioiodinated Fab fragments used in this study are illustrated in Fig. 1. The validity of the new chemical design of antibody fragments in reducing the renal radioactivity levels was estimated.

## MATERIALS AND METHODS

**Reagents and Chemicals.** Na[$^{131}$I]I and Na[$^{125}$I]I were obtained from Daiichi Radioisotope Laboratories (Tokyo, Japan) and Daiichi Kagaku (Tokyo, Japan), respectively, and were diluted with 0.1 M PB (pH 7.4) to 37 MBq (1 mCi)/2–10 $\mu$l. The stannyl precursors of the radioiodination reagents, SHML, SMPH, and SMIH, were synthesized as reported previously (25, 26). Size-exclusion HPLC and RP-HPLC were performed using Cosmosil Diol-300 (7.5 $\times$ 600 mm, Nacalai Tesque, Kyoto, Japan) and Cosmosil 5C$_{18}$-AR (4.6 $\times$ 250 mm, Nacalai Tesque) columns, respectively. Size-exclusion HPLC and RP-HPLC columns were equilibrated and eluted with 0.1 M PB (pH 6.8) and with a mixture of 0.1% aqueous phosphoric acid and acetonitrile (7:3), respectively, at a flow rate of 1 ml/min. Other reagents were of reagent grade and were used as received.

**Tumor and mAb.** KT005-cloned human osteogenic sarcoma was maintained by serial s.c. transplantation in athymic mice. Pieces of tumor tissue (~0.5 g) at ~2.5 weeks postimplantation were used for the *in vivo* study. The mAb against osteogenic sarcoma (OST7, IgG1), generated by the standard hybridoma technique, was purified by ammonium sulfate precipitation with subsequent protein A affinity chromatography (Pharmacia Biotech Co. Ltd., Tokyo, Japan), as reported previously (29). The Fab fragment was prepared by the standard procedure using papain (30).

**Preparation of Radioiodinated Fab Fragments.** SHML, SMPH, and SMIH were radioiodinated in the presence of NCS as described previously (26). Briefly, SHML was dissolved in methanol containing 1% AcOH (0.64 mg/ml), and 8.4 $\mu$l (0.021 $\mu$mol) of this solution were mixed with 2.3 $\mu$l of NCS in methanol (0.5 mg/ml) in a sealed vial, followed by addition of Na[$^{131}$I]I (1 $\mu$l). After incubation at room temperature for 25 min, the reaction was quenched with aqueous sodium bisulfite (1.1 $\mu$l, 0.72 mg/ml). The radiochemical yield of [$^{131}$I]HML was determined by silica gel TLC (Merck Art 5553) developed with a mixture of chloroform, methanol, and AcOH (40:5:2). The solvent was removed under a stream of $N_2$ prior to subsequent conjugation reaction with the Fab fragment.

Conjugation of [$^{131}$I]HML with the Fab fragment of OST7 was performed by treating the Fab fragment with 2-IT, followed by the conjugation reaction between the thiol groups of Fab and the maleimide groups of [$^{131}$I]HML (26). Briefly, a solution of Fab (200 $\mu$l, 2 mg/ml) in well-degassed 0.16 M BB (pH 8.0) containing 2 mM EDTA was allowed to react with 7.2 $\mu$l of 2-IT solution (1 mg/ml) prepared in the same buffer. After gentle agitation of the reaction mixture for 60 min at room temperature, excess 2-IT was removed by a centrifuged column procedure (31) using Sephadex G-50 (Pharmacia Biotech Co. Ltd.) equilibrated and eluted with 0.1 M PB (pH 6.0) containing 2 mM EDTA. Aliquots of this mixture were sampled for estimation of the number of thiol groups with 2,2′-dipyridyl disulfide (32). The filtrate (100 $\mu$l) was then added to a reaction vial containing crude [$^{131}$I]HML. After gentle agitation of the reaction mixture for 1.5 h at room temperature, 14.8 $\mu$l of iodoacetamide (10 mg/ml) in 0.1 M PB (pH 6.0) were added. The reaction mixture was further incubated for 30 min to alkylate the unreacted thiol groups. [$^{131}$I]HML-Fab was subsequently purified by the centrifuged column procedure, equilibrated, and eluted with 0.1 M acetate buffer (pH 6.0).

[$^{125}$I]MIH-Fab and [$^{125}$I]MPH-Fab were also prepared by experimental procedures similar to those used for [$^{131}$I]HML-Fab, except that SMIH or SMPH was used in place of SHML, as reported previously (25, 26).

Direct radioiodination of Fab was performed by the chloramine T method (23). To 100-$\mu$l aliquots of Fab (2.5 mg/ml) in 0.3 M PB (pH 7.3) was added 1 $\mu$l of Na[$^{125}$I]I. Chloramine T (0.1 mg/ml, 12.5 $\mu$l), freshly prepared in the same buffer, was then added. After incubation of the mixture for 5 min at room temperature, $^{125}$I-Fab was purified by the centrifuged column procedure, as described above.

Radiochemical purities of the radioiodinated Fab fragments were determined by size-exclusion HPLC and silica gel TLC developed with a mixture of methanol and water (4:1).

**Stability of Radioiodinated Fab Fragments in Human Serum.** Each radiolabeled Fab fragment was diluted to 0.5 mg/ml with 0.1 M PB (pH 6.0), and 20 $\mu$l of each solution were added to 230 $\mu$l of freshly prepared human serum. After incubation for 1, 3, 6, 24, or 48 h at 37°C, samples were taken from the solutions, and the percentages of radioactivity released from each antibody were determined by paper chromatography (No. 50; Advantec Toyo, Tokyo, Japan) and silica gel TLC. Each value was calculated by dividing the antibody-bound radioactivity at various intervals by the radiochemical purity of freshly prepared respective antibody. Paper chromatography was developed with a mixture of methanol and water (4:1). Under these conditions, protein-bound radioactivity, free iodine, *m*-iodobenzoic acid, and *m*-iodohippuric acid had $R_f$s of 0, 0.6–0.65, 0.9–0.95, and 0.9–0.95, respectively. TLC plates were developed with a mixture of chloroform, methanol, and water (15:8:1). Under these conditions, protein-bound radioactivity, free iodine, *meta*-iodohippuric acid, and *meta*-iodobenzoic acid had $R_f$s of 0, 0.1, 0.25, and 0.4, respectively.

**Biodistribution of Radioiodinated Fab Fragments.** *In vivo* studies were performed after simultaneous administration of a mixed solution of [$^{131}$I]HML-Fab and [$^{125}$I]MIH-Fab, [$^{125}$I]MPH-Fab, or $^{125}$I-Fab. Three ml of 0.1 M PB (pH 6.0) containing 600 $\mu$g of unmodified Fab were mixed with 10 $\mu$l each of [$^{131}$I]HML-Fab (12 $\mu$Ci) and [$^{125}$I]MIH-Fab (13 $\mu$Ci), [$^{125}$I]MPH-Fab (13 $\mu$Ci), or $^{125}$I-Fab (13 $\mu$Ci) prior to administration. The biodistribution of radioactivity after i.v. administration of each mixture to 6-week-old ddY mice (33) was monitored at 10 and 30 min and 1, 3, 6, and 24 h postinjection. Groups of five mice, each receiving 20 $\mu$g of Fab fragments, were used for the experiments. Organs of interest were removed and weighed, and the radioactivity was determined with a well counter (ARC 2000; Aloka, Tokyo, Japan). A window from 29 to 97 keV was used for counting $^{125}$I, whereas one from 280 to 440 keV was used for $^{131}$I. Correlation factors to eliminate cross-over of $^{131}$I activity into $^{125}$I were determined by counting $^{131}$I standard in each window. The crossover of $^{125}$I into the $^{131}$I channel was negligible. To determine the amounts and routes of radioactivity excretion from the body, mice were housed in metabolic cages (Metabolica MM type; Sugiyama-Gen Iriki Co. Ltd., Tokyo, Japan) for 24 h after administration of the respective preparation. Urine and feces were collected for 6 and 24 h postinjection, and the radioactivities were determined.

The radiolabeled species excreted in the urine for 6 h postinjection of



Downloaded from http://aacrjournals.org/cancerres/article-pdf/59/1/128/3228790/ch0199001280.pdf by guest on 05 November 2024

[$^{131}$I]HML-Fab were immediately analyzed by silica gel TLC developed with a mixture of chloroform, methanol, and water (15:8:1) before and after filtration through a $M_r$ 10,000 cutoff ultrafiltration membrane (Microcon 10; Amicon Grace, Tokyo, Japan). The urine samples were also analyzed by size-exclusion HPLC and RP-HPLC after filtration through a polycarbonate membrane with a pore diameter of 0.45 $\mu$m (Cosmonice Filter, Nacalai Tesque) and a $M_r$ 10,000 cutoff ultrafiltration membrane, respectively. On RP-HPLC analysis, free iodine, *meta*-iodohippuric acid, and *meta*-iodobenzoic acid had retention times of 3, 9, and 31 min, respectively.

Athymic mice bearing osteogenic sarcoma were also treated i.v. with 100 $\mu$l of a mixed solution of [$^{131}$I]HML-Fab and $^{125}$I-Fab, prepared as described above. The animals were sacrificed at 3 h postinjection (six mice). Organs of interest were removed and weighed, and the radioactivity in each tissue was determined (ARC-2000).

**Subcellular Distribution of the Radioactivity.** The subcellular distribution of the radioactivity in the kidney was determined 10 and 30 min after administration of 20 $\mu$g each of [$^{131}$I]HML-Fab, [$^{125}$I]MIH-Fab, or $^{125}$I-Fab, according to the procedures described previously, with slight modifications (34). At the indicated times, murine kidneys were isolated, minced, and homogenized in 4 volumes of ice-cold 0.25 M sucrose containing 1 mM EDTA with a Dounce homogenizer by hand (20 strokes). This was followed by two final strokes in an ice-cold Potter-Elvehjem homogenizer with a Teflon pestle rotated at 800 rpm. The resulting 20% homogenate was centrifuged twice for 5 min at 340 $\times$ *g* at 4°C. The isolated supernatant was layered on top of iso-osmotic (0.25 M sucrose) Percoll (Pharmacia Biotech Co. Ltd.) at a density of 1.08 g/ml. After centrifugation at 20,000 $\times$ *g* (RP 30 rotor: Hitachi Co. Ltd., Tokyo, Japan) for 90 min at 4°C, the gradient (~1.02–1.14 g/ml) was collected in 14 fractions before analyses of $\beta$-galactosidase (35), alkaline phosphodiesterase I activities (36), density, and the radioactivity of each fraction.

**Statistical Analysis.** Data are expressed as means ± SD where appropriate. Results were statistically analyzed using the unpaired Mann-Whitney test. Differences were considered statistically significant when $P$ was $<0.05$.

## RESULTS

**Preparation of Radiolabeled Fab Fragments.** Radioiodination of SHML was performed in the presence of NCS as an oxidant. [$^{131}$I]HML was obtained with a radiochemical yield of 67.2%, as determined by TLC. Similar procedures were used for the preparation of [$^{125}$I]MIH and [$^{125}$I]MPH with radiochemical yields of 68.9 and 71.2%, respectively. All of the radioiodinated compounds were treated with sodium bisulfite to quench any residual NCS, preventing the iodine species from reacting with tyrosine residues of the antibody molecule. Neutralization of NCS also prevented exposure of the protein to the oxidant.

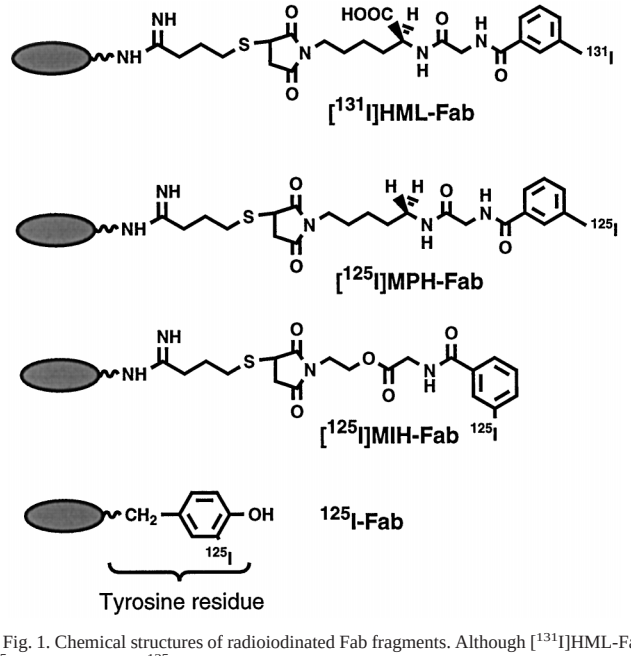


Fig. 1. Chemical structures of radioiodinated Fab fragments. Although [$^{131}$I]HML-Fab, [$^{125}$I]MPH-Fab, and [$^{125}$I]MIH-Fab were prepared with similar conjugation chemistry, $^{125}$I-Fab was prepared by direct iodination of Fab in the presence of chloramine T.

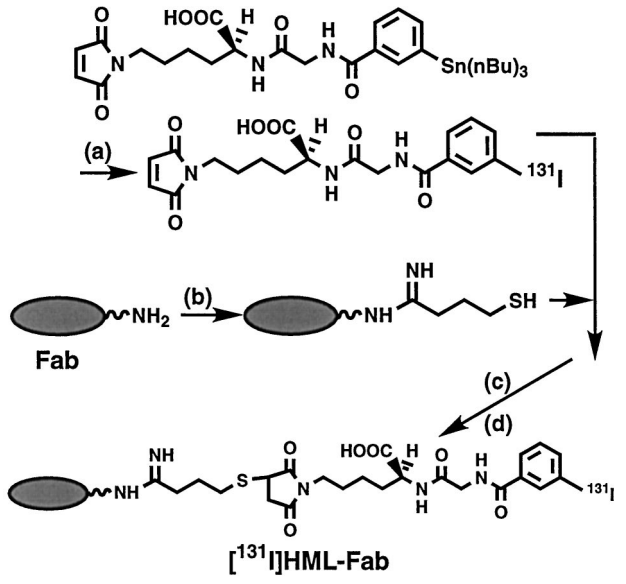


Fig. 2. Conjugation of [$^{131}$I]HML with Fab fragments. Reagents: *(a)*, NCS, Na[$^{131}$I]I, and 1% AcOH/MeOH; *(b)*, 2-IT and 0.1 M BB (pH 8.0)-2 mM EDTA; *(c)*, 0.1 M PB (pH 6.0); and *(d)*, iodoacetamide.

Conjugation of [$^{131}$I]HML with Fab fragments was performed by reacting the thiolated Fab fragments with the maleimide groups of [$^{131}$I]HML, as shown in Fig. 2. A preliminary study showed that only the thiol groups of Fab reacted with the maleimide groups and that the alkylation of lysine residues with maleimide was negligible or nonexistent under these conditions (37). Treatment of Fab fragments with 2-IT introduced ~2.4 mol of thiol groups per molecule of Fab, as determined using 2,2′-dipyridyl disulfide. The radiochemical yield of [$^{131}$I]HML-Fab was 35.1%, as determined by TLC. After purification by the centrifuged column procedure, [$^{131}$I]HML-Fab was obtained with a radiochemical purity and specific activity of 95.8% and 575 $\mu$Ci/mg, respectively, as determined by size-exclusion HPLC. [$^{125}$I]MPH-Fab and [$^{125}$I]MIH-Fab were obtained with radiochemical yields of 36.7 and 36.4%, respectively. Radiochemical purities and specific activities were 99.7% and 625 $\mu$Ci/mg, respectively, for [$^{125}$I]MPH-Fab, whereas those for [$^{125}$I]MIH-Fab were 99.5% and 650 $\mu$Ci/mg. $^{125}$I-Fab was prepared by the chloramine T method with radiochemical purity and specific activity of 94.9% and 640 $\mu$Ci/mg, respectively.

**Serum Stability of Radiolabeled Fab Fragments.** [$^{131}$I]HML-Fab, [$^{125}$I]MPH-Fab, and $^{125}$I-Fab released only 2–3% of the initial antibody-bound radioactivity, even after incubation in freshly prepared human serum at 37°C for 48 h. However, [$^{125}$I]MIH-Fab released radioactivity as *meta*-iodohippuric acid in a time-dependent manner, and 81.6, 44.4, and 22.0% of the initial antibody-bound radioactivity were detected in the protein fractions after 3, 24, and 48 h of incubation, respectively.

***In Vivo* Studies.** The biodistributions of the radioactivity after simultaneous administration of [$^{131}$I]HML-Fab and [$^{125}$I]MPH-Fab to normal mice are summarized in Table 1. No significant differences were observed in the blood radioactivity levels between the two radioiodinated Fab fragments. However, although [$^{125}$I]MPH-Fab showed high radioactivity levels in the kidney and reached its peak at 1 h, [$^{131}$I]HML-Fab showed significantly lower renal radioactivity



Downloaded from http://aacrjournals.org/cancerres/article-pdf/59/1/128/3228790/ch0199001280.pdf by guest on 05 November 2024

Table 1 *Biodistributions of radioactivity in mice after injection of [$^{131}$I]HML-Fab and [$^{125}$I]MPH-Fab*

Tissue radioactivity is expressed as % ID/g [for each group, $n = 5$; results are reported as mean (SD)].

| | Time after injection | | | | | |
|---|---|---|---|---|---|---|
| | 10 min | 30 min | 1 h | 3 h | 6 h | 24 h |
| [$^{131}$I]HML-Fab | | | | | | |
| Blood | 22.27 (2.20) | 14.05 (1.32) | 9.19 (0.52) | 4.24 (0.34) | 1.90 (0.26) | 0.35 (0.08) |
| Liver | 4.75 (0.66) | 3.20 (0.36) | 2.17 (0.13) | 1.11 (0.13) | 0.66 (0.10) | 0.18 (0.05) |
| Kidney | 20.35 (0.42) | 10.99 (1.59) | 7.08 (0.49) | 3.43 (0.92) | 1.61 (0.32) | 0.20 (0.03) |
| Intestine | 0.77 (0.13) | 1.23 (0.13) | 1.37 (0.09) | 1.24 (0.12) | 0.97 (0.16) | 0.07 (0.01) |
| Spleen | 3.17 (0.52) | 2.23 (0.25) | 1.45 (0.21) | 0.79 (0.08) | 0.36 (0.09) | 0.04 (0.04) |
| Stomach[a] | 0.53 (0.03) | 0.69 (0.05) | 0.69 (0.11) | 0.59 (0.03) | 0.66 (0.18) | 0.08 (0.01) |
| Urine[a] | | | | | 45.99 (3.18) | 68.23 (3.16) |
| Feces[a] | | | | | 0.71 (0.33) | 2.86 (0.69) |
| [$^{125}$I]MPH-Fab | | | | | | |
| Blood | 22.51 (2.24) | 15.13 (1.54) | 9.33 (0.51) | 4.06 (0.23) | 1.83 (0.24) | 0.33 (0.07) |
| Liver | 4.44 (0.54) | 3.54 (0.41) | 3.03[b] (0.18) | 1.85[b] (0.32) | 1.20[b] (0.22) | 0.11[c] (0.03) |
| Kidney | 39.88[c] (2.53) | 61.11[b] (8.13) | 65.51[b] (3.06) | 53.18[b] (4.89) | 31.05[b] (3.17) | 1.42[b] (0.67) |
| Intestine | 0.89 (0.14) | 1.52[c] (0.15) | 2.24[b] (0.08) | 3.71[b] (0.53) | 4.52[c] (0.60) | 0.31[c] (0.06) |
| Spleen | 3.27 (0.47) | 2.24 (0.17) | 1.62 (0.31) | 0.86 (0.16) | 0.44 (0.23) | 0.39 (0.05) |
| Stomach[a] | 0.54 (0.06) | 0.69 (0.07) | 0.71 (0.18) | 0.84[b] (0.10) | 0.92 (0.19) | 0.29 (0.18) |
| Urine[a] | | | | | 36.24 (1.38) | 57.55 (1.19) |
| Feces[a] | | | | | 0.58 (0.33) | 11.50 (0.58) |

[a] Expressed as % ID.
[b] Significance determined by unpaired Mann-Whitney test; $P < 0.01$ compared to [$^{131}$I]HML-Fab.
[c] Significance determined by unpaired Mann-Whitney test; $P < 0.05$ compared to [$^{131}$I]HML Fab.

levels at all postinjection time points examined. The biodistributions of the radioactivity after concomitant injection of [$^{131}$I]HML-Fab and $^{125}$I-Fab are shown in Table 2. Although [$^{131}$I]HML-Fab showed slightly higher radioactivity levels in the blood, [$^{131}$I]HML-Fab demonstrated significantly lower radioactivity levels in the kidney than $^{125}$I-Fab from 10 min postinjection onward. $^{125}$I-Fab showed the highest radioactivity levels in the kidney at 30 min postinjection. Table 3 shows the localizations of the radioactivity after concomitant administration of [$^{131}$I]HML-Fab and [$^{125}$I]MIH-Fab. Although [$^{131}$I]HML-Fab showed slightly slower elimination rates of the radioactivity from the blood, [$^{131}$I]HML-Fab demonstrated significantly lower levels of radioactivity in the kidney at early postinjection time points as compared with [$^{125}$I]MIH-Fab. The kidney:blood ratios of the radioactivity in the three experiments are summarized in Fig. 3. [$^{125}$I]MPH-Fab showed the highest kidney:blood ratios of radioactivity, reaching a peaked ratio of 16.9 at 6 h postinjection. Although [$^{125}$I]MIH-Fab showed lower kidney:blood ratios than those of $^{125}$I-Fab throughout the experimental period, both [$^{125}$I]MIH-Fab and $^{125}$I-Fab reached their peak ratios of 3.8 and 7.3, respectively, at 1 h postinjection. On the other hand, [$^{131}$I]HML-Fab demonstrated almost constant radioactivity ratios of ~1 from 10 min to 3 h postinjection, and the ratios were significantly lower than those observed with [$^{125}$I]MIH-Fab.

Fig. 4 shows the radiochromatograms of urine samples obtained for 6 h postinjection of [$^{131}$I]HML-Fab when analyzed by size-exclusion HPLC (Fig. 4*A*) and TLC (Fig. 4*B*). On size-exclusion HPLC, the majority of the radioactivity (85.5%) was observed in the LMW fractions with ~12% of the radioactivity being eluted in fractions similar to those of intact [$^{131}$I]HML-Fab. On TLC analysis, 14.6% of the radioactivity was detected at the origin and 84.4% of the radioactivity was observed with an $R_f$ of 0.25. Fig. 4, *C* and *D*, show RP-HPLC and TLC radiochromatograms of urine samples after filtration through a $M_r$ 10,000 cutoff membrane. On RP-HPLC, 93.0% of the radioactivity of the urine samples was observed with a retention time of 9 min, identical to that of *meta*-iodohippuric acid. On TLC analysis, 97.9% of the radioactivity in the urine samples was detected with an $R_f$ of 0.25, identical to that of *meta*-iodohippuric acid. On analysis of urine samples obtained 6 h postinjection of [$^{125}$I]MIH-Fab,

Table 2 *Biodistributions of radioactivity in mice after injection of [$^{131}$I]HML-Fab and $^{125}$I-Fab*

Tissue radioactivity is expressed as % ID/g [for each group, $n = 5$; results are reported as mean (SD)].

| | Time after injection | | | | | |
|---|---|---|---|---|---|---|
| | 10 min | 30 min | 1 h | 3 h | 6 h | 24 h |
| [$^{131}$I]HML-Fab | | | | | | |
| Blood | 21.88 (1.37) | 14.94 (1.13) | 9.46 (0.36) | 4.87 (0.97) | 2.33 (0.13) | 0.38 (0.05) |
| Liver | 5.29 (0.26) | 3.54 (0.14) | 2.51 (0.08) | 1.24 (0.13) | 0.80 (0.11) | 0.17 (0.01) |
| Kidney | 21.39 (1.19) | 12.51 (1.55) | 9.35 (1.86) | 2.74 (0.39) | 1.62 (0.34) | 0.20 (0.04) |
| Intestine | 0.88 (0.13) | 1.27 (0.09) | 1.53 (0.13) | 1.42 (0.16) | 1.11 (0.13) | 0.08 (0.02) |
| Spleen | 3.42 (0.37) | 2.30 (0.33) | 1.68 (0.13) | 0.77 (0.10) | 0.55 (0.11) | 0.13 (0.09) |
| Stomach[a] | 0.52 (0.07) | 0.65 (0.11) | 0.82 (0.08) | 0.94 (0.16) | 0.64 (0.21) | 0.10 (0.04) |
| Urine[a] | | | | | 46.88 (8.50) | 71.40 (3.50) |
| Feces[a] | | | | | 0.03 (0.02) | 2.73 (0.59) |
| $^{125}$I-Fab | | | | | | |
| Blood | 19.29 (1.43) | 11.05[b] (1.31) | 6.72[b] (0.26) | 3.43[c] (0.34) | 2.32 (0.49) | 0.29 (0.06) |
| Liver | 3.70[b] (0.23) | 2.37[b] (0.11) | 1.83[b] (0.12) | 1.11 (0.12) | 0.84 (0.14) | 0.18 (0.02) |
| Kidney | 53.21[b] (2.56) | 64.55[c] (4.52) | 48.80[b] (4.52) | 16.28[b] (5.33) | 5.83[b] (1.08) | 0.51[b] (0.07) |
| Intestine | 0.98 (0.14) | 1.38 (0.08) | 1.74 (0.11) | 1.44[c] (0.14) | 1.27 (0.23) | 0.14 (0.04) |
| Spleen | 3.64 (0.66) | 2.94 (0.77) | 2.31[c] (0.37) | 1.77[b] (0.27) | 1.26[b] (0.35) | 0.29 (0.18) |
| Stomach[a] | 0.86[b] (0.09) | 2.32[b] (0.44) | 7.26[b] (1.23) | 12.94[b] (1.19) | 10.56[b] (2.33) | 0.44[b] (0.23) |
| Urine[a] | | | | | 31.80 (4.02) | 63.96 (5.08) |
| Feces[a] | | | | | 0.01 (0.02) | 2.73 (0.59) |

[a] Expressed as % ID.
[b] Significance determined by unpaired Mann-Whitney test; $P < 0.01$ compared to [$^{131}$I]HML-Fab.
[c] Significance determined by unpaired Mann-Whitney test; $P < 0.05$ compared to [$^{131}$I]HML-Fab.



Downloaded from http://aacrjournals.org/cancerres/article-pdf/59/1/128/3228790/ch0199000128o.pdf by guest on 05 November 2024

Table 3 *Biodistributions of radioactivity in mice after injection of [$^{131}$I]HML-Fab and [$^{125}$I]MIH-Fab*

Tissue radioactivity is expressed as % ID/g [for each group, $n = 5$; results are reported as mean (SD)].

| | Time after injection | | | | | |
|---|---|---|---|---|---|---|
| | 10 min | 30 min | 1 h | 3 h | 6 h | 24 h |
| [$^{131}$I]HML-Fab | | | | | | |
| Blood | 22.54 (1.37) | 15.77 (1.03) | 9.46 (1.25) | 4.46 (0.56) | 1.93 (0.18) | 0.34 (0.08) |
| Liver | 4.94 (0.53) | 3.51 (0.29) | 2.13 (0.27) | 1.11 (0.11) | 0.65 (0.11) | 0.18 (0.03) |
| Kidney | 28.39 (2.85) | 14.06 (1.69) | 7.97 (0.77) | 2.87 (0.37) | 1.38 (0.20) | 0.18 (0.03) |
| Intestine | 0.91 (0.06) | 1.41 (0.13) | 1.51 (0.33) | 1.39 (0.14) | 1.08 (0.15) | 0.11 (0.07) |
| Spleen | 3.69 (0.70) | 2.80 (0.42) | 1.59 (0.23) | 0.96 (0.16) | 0.41 (0.05) | 0.02 (0.02) |
| Stomach[a] | 0.41 (0.06) | 0.73 (0.13) | 1.05 (0.15) | 0.88 (0.16) | 0.51 (0.18) | 0.07 (0.05) |
| Urine[a] | | | | | 43.71 (3.11) | 68.98 (5.52) |
| Feces[a] | | | | | 0.90 (1.13) | 2.41 (2.55) |
| [$^{125}$I]MIH-Fab | | | | | | |
| Blood | 19.84[b] (0.74) | 12.33[c] (0.74) | 6.67[b] (0.85) | 3.03[c] (0.45) | 1.31[b] (0.12) | 0.21[b] (0.04) |
| Liver | 3.80[b] (0.42) | 2.55[c] (0.21) | 1.37[b] (0.13) | 0.57[c] (0.04) | 0.31[b] (0.05) | 0.06[c] (0.03) |
| Kidney | 51.31[b] (4.18) | 39.34[c] (3.15) | 25.38[b] (4.23) | 5.79[c] (1.26) | 1.46 (0.28) | 0.15 (0.03) |
| Intestine | 0.87 (0.08) | 1.14[b] (0.09) | 1.00 (0.22) | 0.59[c] (0.05) | 0.33[b] (0.04) | 0.04 (0.01) |
| Spleen | 3.29 (0.73) | 2.46 (0.30) | 1.55 (0.64) | 0.75 (0.12) | 0.36 (0.18) | 0.17 (0.16) |
| Stomach[a] | 0.48 (0.06) | 0.73 (0.06) | 1.10 (0.27) | 0.73 (0.14) | 0.46 (0.84) | 0.16 (0.13) |
| Urine[a] | | | | | 53.48 (3.06) | 76.01 (5.99) |
| Feces[a] | | | | | 1.07 (1.43) | 2.41 (2.55) |

[a] Expressed as % ID.
[b] Significance determined by unpaired Mann-Whitney test; $P < 0.05$ compared to [$^{131}$I]HML-Fab.
[c] Significance determined by unpaired Mann-Whitney test; $P < 0.01$ compared to [$^{131}$I]HML-Fab.

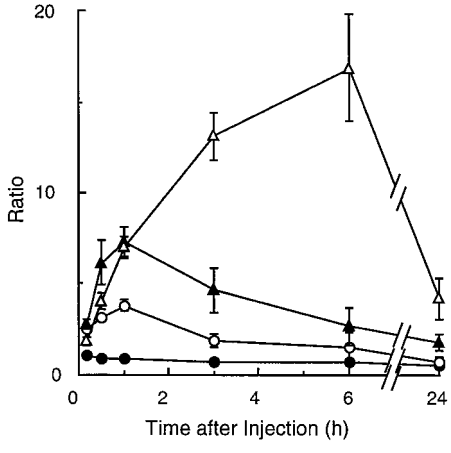


Fig. 3. Kidney:blood ratios of the radioactivity after administration of [$^{131}$I]HML-Fab (●), [$^{125}$I]MIH-Fab (○), [$^{125}$I]MPH-Fab (△), and $^{125}$I-Fab (▲) to normal mice. Kidney:blood ratios of [$^{131}$I]HML-Fab are presented as averages of the three experiments ($n = 15$). Significance was determined by unpaired Mann-Whitney test. [$^{131}$I]HML-Fab *versus* $^{125}$I-Fab, $P < 0.01$ at 10 and 30 min and 1, 3, 6, and 24 h; [$^{131}$I]HML-Fab *versus* [$^{125}$I]MPH-Fab, $P < 0.01$ at 10 and 30 min and 1, 3, 6, and 24 h; [$^{131}$I]HML-Fab *versus* [$^{125}$I]MIH-Fab, $P < 0.01$ at 10 and 30 min and 3 h and $P < 0.05$ at 1 and 6 h.

>95% of the radioactivity of the LMW fractions was detected at a position identical to that of *meta*-iodohippuric acid (data not shown).

The biodistributions of radioactivity after simultaneous administration of [$^{131}$I]HML-Fab and $^{125}$I-Fab in nude mice bearing osteogenic sarcoma are summarized in Fig. 5. [$^{131}$I]HML-Fab showed significantly lower radioactivity levels in the kidney than of $^{125}$I-Fab, whereas no significant differences were observed in the radioactivity levels in the tumor between the two radioiodinated Fab fragments. As a result, [$^{131}$I]HML-Fab increased the tumor:kidney ratios of the radioactivity by a factor of ~4.

**Subcellular Distribution of Radioactivity.** Percoll density gradient centrifugation profiles of the radioactivity at 10 and 30 min postinjection of [$^{131}$I]HML-Fab, [$^{125}$I]MIH-Fab, and $^{125}$I-Fab are illustrated in Fig. 6. Both [$^{125}$I]MIH-Fab and $^{125}$I-Fab showed two radioactivity peaks at densities of 1.04–1.05 and 1.10 g/ml at 10 min postinjection. At 30 min postinjection, the major radioactivity peak was detected at a density of 1.10 g/ml. On the other hand, [$^{131}$I]HML-Fab showed a major radioactivity peak only at the density of 1.04–1.05 g/ml at both 10 and 30 min postinjection. The radioactivity peak at a density of 1.04–1.05 was copurified with alkaline phosphodiesterase I activity, whereas that at a density of ~1.10 was copurified with β-galactosidase activity.

## DISCUSSION

This study was performed to evaluate the hypothesis that the renal radioactivity levels of radiolabeled antibody fragments could be reduced if radiolabeled compounds of urinary excretion were released from the antibody fragments before they were incorporated into renal cells by the action of brush border enzymes present on the lumen of renal tubules. The results with [$^{131}$I]HML-Fab were compared with those of $^{125}$I-Fab, [$^{125}$I]MIH-Fab, and [$^{125}$I]MPH-Fab. [$^{131}$I]HML-Fab, [$^{125}$I]MPH-Fab, and [$^{125}$I]MIH-Fab were prepared with similar conjugation chemistry. Previous studies using galactosyl-neoglycoalbumin and intact IgG showed that [$^{125}$I]MIH-conjugated polypep-

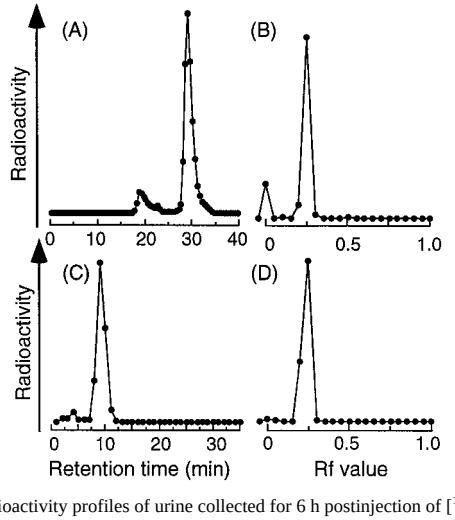


Fig. 4. Radioactivity profiles of urine collected for 6 h postinjection of [$^{131}$I]HML-Fab by size-exclusion HPLC (*A*), TLC (*B* and *D*), and RP-HPLC (*C*). Urine samples were analyzed directly (*B*), after filtration through a polycarbonate membrane with a pore diameter of 0.45 μm (*A*) and after filtration through a $M_r$ 10,000 cutoff membrane (*B* and *D*). On size-exclusion HPLC (*A*) and TLC (*B*), over 85% of the radioactivity was observed in LMW fractions. On RP-HPLC (*C*) and TLC (*D*), 93 and 98% of the LMW fraction showed a retention time or an $R_f$ identical to that of *meta*-iodohippuric acid, respectively.



Downloaded from http://aacrjournals.org/cancerres/article-pdf/59/1/128/3228790/ch0199000128o.pdf by guest on 05 November 2024

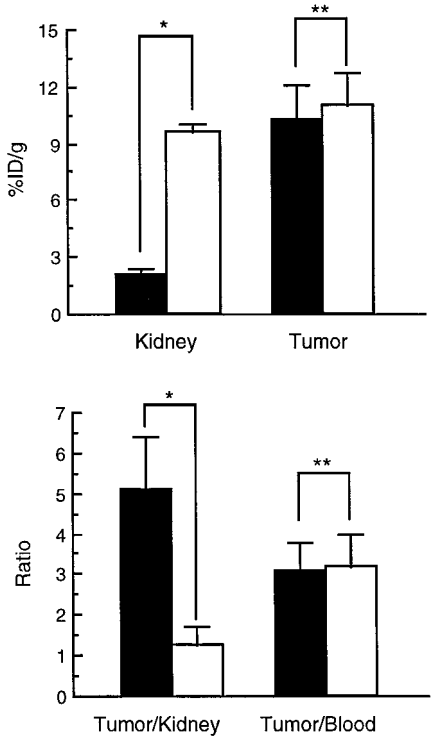


Fig. 5. Biodistribution of radioactivity at 3 h postinjection of [$^{131}$I]HML-Fab (■) and $^{125}$I-Fab (□) into nude mice ($n = 6$) bearing osteogenic sarcoma. *Columns*, means for six mice; *bars*, SD. Mean weights (SD) of mice and tumors in g were 19.21 (1.26) and 0.50 (0.15), respectively. Significance was determined by unpaired Mann-Whitney test (*, $P < 0.005$; **, not significant).

tides released *meta*-iodohippuric acid as the sole radiometabolite after lysosomal proteolysis in hepatic parenchymal cells at a rate similar to that of [$^{131}$I]HML-conjugated polypeptides (23, 25, 26, 28). On the other hand, [$^{125}$I]MPH-conjugated polypeptides generated radiometabolites with long residence times in hepatic parenchymal cells. High resistance against *in vivo* deiodination of HML-, MIH-, and MPH-conjugated polypeptides and their radiometabolites was also confirmed.

Both [$^{131}$I]HML-Fab and [$^{125}$I]MPH-Fab exhibited stable attachment of the radiolabels to the respective protein in serum. This was reflected in the similar radioactivity levels of the two radiolabeled Fab fragments in the blood from 10 min to 24 h postinjection (Table 1). Thus, similar radioactive portions of the radiolabeled Fab fragments would be filtered through the glomerulus and transported to the proximal tubules of the kidney after administration. However, although [$^{125}$I]MPH-Fab reached its peak renal radioactivity of ~65% ID/g at 1 h postinjection, [$^{131}$I]HML-Fab demonstrated markedly lower renal radioactivity levels in a time-dependent manner. [$^{131}$I]HML-Fab also demonstrated significantly lower renal radioactivity levels when compared with simultaneously administered $^{125}$I-Fab that reached its maximum renal radioactivity levels of ~65% ID/g at 30 min postinjection (Table 2). Because >96% of the radioactivity excreted from the body was recovered in the urine (Tables 1–3) and *meta*-[$^{131}$I]iodohippuric acid represented >80% of the radioactivity in the urine after administration of [$^{131}$I]HML-Fab (Fig. 4), the significantly lower renal radioactivity levels achieved by [$^{131}$I]HML-Fab were attributed to the rapid and selective release of *meta*-[$^{131}$I]iodohippuric acid from the Fab fragment in the kidney.

[$^{131}$I]HML-Fab also significantly reduced the renal radioactivity levels even from 10 min postinjection onward, compared with simultaneously administered [$^{125}$I]MIH-Fab (Table 3). This was clearly demonstrated when the kidney:blood ratios of the radioactivity were compared (Fig. 3). Because both HML- and MIH-conjugated polypeptides generated *meta*-iodohippuric acid as radiometabolites at a similar rate after lysosomal proteolysis in hepatocytes (26, 28), similar kidney:blood ratios of the radioactivity would be observed with the two radioiodinated Fab fragments if [$^{131}$I]HML-Fab liberated *meta*-[$^{131}$I]iodohippuric acid after lysosomal proteolysis in the renal cells. Indeed, no significant differences were observed in the liver: blood ratios of the radioactivity after simultaneous administration of [$^{131}$I]HML- and [$^{125}$I]MIH-conjugated intact IgG into mice, although [$^{125}$I]MIH-IgG showed lower radioactivity levels in both the liver and the blood (26, 28). Thus, the significant differences in the kidney: blood ratios of the radioactivity between [$^{131}$I]HML-Fab and [$^{125}$I]MIH-Fab from early postinjection times suggested that [$^{131}$I]HML-Fab would liberate *meta*-[$^{131}$I]iodohippuric acid before the radiolabeled Fab fragment was incorporated and transported to the lysosomal compartment in the renal cells.

To further investigate the low renal radioactivity levels of [$^{131}$I]HML-Fab from early postinjection times, the subcellular localization of the radioactivity was investigated. Although the radioactivity was observed in both membrane and lysosomal fractions at 10 min postinjection of [$^{125}$I]MIH-Fab and $^{125}$I-Fab, the majority of the radioactivity had migrated to the lysosomal fraction after 30 min (Fig. 6). This suggested that most of the administered Fab fragments would be transported to and metabolized in the lysosomal compartment after 30 min injection. This was supported by an increase in the renal radioactivity levels from 10 to 30 min after injection of $^{125}$I-Fab and by the rapid decrease in the renal radioactivity levels of both $^{125}$I-Fab and [$^{125}$I]MIH-Fab from 30 min to 1 h postinjection. Similar maximum renal radioactivity levels of $^{125}$I-Fab at 30 min and [$^{125}$I]MPH-Fab at 1 h postinjection also suggested that lysosomal proteolysis of radiolabeled Fab fragments would proceed 30 min after injection. On the other hand, most of the renal radioactivity after administration of [$^{131}$I]HML-Fab was observed in the membrane fraction at both 10 and 30 min postinjection. In addition, [$^{131}$I]HML-Fab reached its maximum radioactivity levels in the kidney at 10 min postinjection and showed similar kidney:blood radioactivity ratios of ~1 from 10 min to 3 h. These findings implied that [$^{131}$I]HML-Fab released *meta*-[$^{131}$I]iodohippuric acid at the membrane fraction of the renal cells before transported to the lysosomal compartment, presumably by the

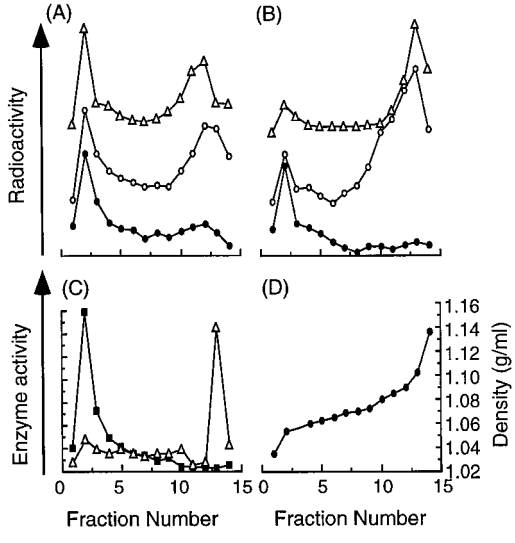


Fig. 6. Subcellular fractionation of the radioactivity in the kidney at 10 min (*A*) and 30 min (*B*) postinjection of [$^{131}$I]HML-Fab (●), [$^{125}$I]MIH-Fab (○), and $^{125}$I-Fab (△). Gradients were collected in 14 fractions from the top of the gradient, assayed for the lysosomal enzyme β-galactosidase (△) and the plasma membrane enzyme alkaline phosphodiesterase I (■; *C*), and measured for density (●; *D*).



Downloaded from http://aacrjournals.org/cancerres/article-pdf/59/1/128/3228790/ch0199001280.pdf by guest on 05 November 2024

action of brush border enzymes present on the lumen of the renal tubules.

The ability of HML to reduce the renal radioactivity levels without impairing the target radioactivity levels delivered by the antibody fragment was demonstrated in the biodistribution study in nude mice (Fig. 5). Although both [$^{131}$I]HML-Fab and $^{125}$I-Fab showed similar radioactivity levels in the tumors, [$^{131}$I]HML-Fab amplified the tumor:kidney ratio of the radioactivity by a factor of ~4, compared with simultaneously administered $^{125}$I-Fab. High stability of the chemical linkage in HML in tumors was also indicated by the unchanged radioactivity levels in the tumor tissue between 24 and 48 h following administration of [$^{131}$I]HML-labeled intact antibody (OST7; Ref. 28). Such chemical and biological characteristics render HML useful as a radioiodination reagent for targeted imaging and targeted therapy using LMW antibody fragments as vehicles although suitable chemistries to improve the radiochemical yields of HML-labeled antibody fragments are required. Because the stannyl precursor of HML, SHML, can be radiofluorinated, HML may also be useful to prepare $^{18}$F-labeled LMW antibody fragments and peptides for PET imaging. Although further studies are required, the findings in this study strongly suggested that renal brush border enzymes may constitute key targets for the radiochemical design of LMW antibody fragments and peptides with low renal radioactivity levels using a variety of clinically important radionuclides.

## ACKNOWLEDGMENTS

We are grateful to Dr. Isamu Yomoda of Diichi Radioisotope Laboratories (Tokyo, Japan) for providing Na[$^{131}$I]I.

## REFERENCES

1. Yokota, T., Milenic, D. E., Whitlow, M., Wood, J. F., Hubert, S. L., and Schlom, J. Microautoradiographic analysis of the normal organ distribution of radioiodinated single-chain Fv and other immunoglobulin forms. Cancer Res., *53:* 3776–3783, 1993.
2. Buijs, W. C. A. M., Massuger, L. F. A. G., Claessens, R. A. M. J., Kenemans, P., and Corstens, F. H. M. Dosimetric evaluation of immunoscintigraphy using indium-111-labeled monoclonal antibody fragments in patients with ovarian cancer. J. Nucl. Med., *33:* 1113–1120, 1992.
3. Baum, R. P., Niesen, A., Hertel, A., Adams, S., Kojouharoff, G., Goldenberg, D. M., and Hor, G. Initial clinical results with technetium-99m-labeled Ll2 monoclonal antibody fragment in the radioimmunodetection of B-cell lymphomas. Cancer (Phila.), *73:* 896–899, 1994.
4. Behr, T. M., Becker, W. S., Bair, H. J., Klein, M. W., Stuhler, C. M., Cidlinsky, K. P., Wittekind, C. W., Scheele, J. R., and Wolf, F. G. Comparison of complete *versus* fragmented technetium-99m-labeled anti-CEA monoclonal antibodies for immunoscintigraphy in colorectal cancer. J. Nucl. Med., *36:* 430–441, 1995.
5. Choi, C. W., Lang, L., Lee, J. T., Webber, K. O., Yoo, T. M., Chang, H. K., Le, N., Jagoda, E., Paik, C. H., Pastan, I., Eckelman, W. C., and Carrasquillo, J. A. Biodistribution of F-18- and I-125-labeled anti-Tac disulfide-stabilized Fv fragments in nude mice with interleukin 2$\alpha$ receptor-positive tumor xenografts. Cancer Res., *55:* 5323–5329, 1995.
6. Wu, C., Jagoda, E., Brechbiel, M., Webber, K. O., Pastan, I., Gansow, O., and Eckelman, W. C. Biodistribution and catabolism of Ga-67-labeled anti-Tac dsFv fragment. Bioconjugate Chem., *8:* 365–369, 1997.
7. Wochner, D., Strober, W., and Waldmann, T. A. The role of the kidney in the catabolism of bence jones proteins and immunoglobulin fragments. J. Exp. Med., *126:* 207–221, 1967.
8. Arend, W. P., and Silverblatt, F. J. Serum disappearance and catabolism of homologous immunoglobulin fragments in rats. Scand. J. Clin. Lab. Invest., *37:* 502–513, 1975.
9. Carone, F. A., Peterson, D. R., Oparil, S., and Pullman, T. N. Renal tubular transport and catabolism of proteins and peptides. Kidney Int., *16:* 271–278, 1979.
10. Maack, T., Johnson, V., Kau, S. T., Figueiredo, J., and Sigulem, D. Renal filtration, transport, and metabolism of low-molecular-weight proteins: a review. Kidney Int., *16:* 251–270, 1979.
11. Silberbagl, S. The renal handling of amino acids and oligopeptides. Physiol. Rev., *68:* 811–1007, 1988.
12. Franssen, E. J. F., Moolenaar, F., Dezeeuw, D., and Meijer, D. K. F. Low molecular weight proteins as carriers for renal drug targeting: Naproxen coupled to lysozyme via the spacer L-lactic acid. Pharm. Res., *10:* 963–969, 1993.
13. Simonnet, H., Gauthier, C., Gire, V., and Baverel, G. Protein endocytosis by a kidney tubule suspension: metabolic requirements. Biochim. Biophys. Acta, *1189:* 152–162, 1994.
14. Schott, M. E., Milenic, D. E., Yokota, T., Whitlow, M., Wood, J. F., Fordyce, W. A., Cheng, R. C., and Schlom, J. Differential metabolic patterns of iodinated *versus* radiometal chelated anticarcinoma single-chain-Fv molecules. Cancer Res., *52:* 6413–6417, 1992.
15. Rogers, B. E., Franano, F. N., Duncan, J. R., Edwards, W. B., Anderson, C. J., Connett, J. M., and Welch, M. J. Identification of metabolites of In-111-diethylenetriaminepentaacetic acid monoclonal antibodies and antibody fragments *in vivo*. Cancer Res., *55* (Suppl.)*:* S5714–S5720, 1995.
16. Rogers, B. E., Anderson, C. J., Connett, J. M., Guo, L. W., Edwards, W. B., Sherman, E. L. C., Zinn, K. R., and Welch, M. J. Comparison of four bifunctional chelates for radiolabeling monoclonal antibodies with copper radioisotopes: biodistribution and metabolism. Bioconjugate Chem., *7:* 511–522, 1996.
17. Behr, T. M., Sharkey, R. M., Juweid, M. E., Blumenthal, R. D., Dunn, R. M., Griffiths, G. L., Bair, H. J., Wolf, F. G., Becker, W. S., and Goldenberg, D. M. Reduction of the renal uptake of radiolabeled monoclonal antibody fragments by cationic amino acids and their derivatives. Cancer Res., *55:* 3825–3834, 1995.
18. Behr, T. M., Becker, W. S., Sharkey, R. M., Juweid, M. E., Dunn, R. M., Bair, H. J., Wolf, F. G., and Goldenberg, D. M. Reduction of renal uptake of monoclonal antibody fragments by amino acid infusion. J. Nucl. Med., *37:* 829–833, 1996.
19. Kobayashi, H., Yoo, T. M., Kim, I. S., Kim, M. K., Le, N., Webber, K. O., Pastan, I., Paik, C. H., Eckelman, W. C., and Carrasquillo, J. A. L-Lysine effectively blocks renal uptake of I-125- or Tc-99m-labeled anti-Tac disulfide-stabilized Fv fragment. Cancer Res., *56:* 3788–3795, 1996.
20. Zanger, R. A. Amino acid hyperalimentation in acute renal failure: a potential therapeutic paradox. Kidney Int., *32* (Suppl. 22)*:* S72–S75, 1987.
21. Weber, R. W., Boutin, R. H., Nedelman, M. A., Lister-James, J., and Dean, R. T. Enhanced kidney clearance with an ester-linked $^{99m}$Tc-radiolabeled antibody Fab′-chelator conjugate. Bioconjugate Chem., *1:* 431–437, 1990.
22. Bridger, G. J., Abrams, M. J., Padmanabhan, S., Gaul, F., Larsen, S., Henson, G. W., Schwartz, D. A., Longley, C. B., Burton, C. A., and Ultee, M. E. A Comparison of cleavable and noncleavable hydrazinopyridine linkers for the $^{99m}$Tc labeling of Fab′ monoclonal antibody fragments. Bioconj. Chem., *7:* 255–264, 1996.
23. Arano, Y., Wakisaka, K., Ohmomo, Y., Uezono, T., Akizawa, H., Nakayama, M., Sakahara, H., Tanaka, C., Konishi, J., and Yokoyama, A. Assessment of radiochemical design of antibodies using an ester bond as the metabolizable linkage: Evaluation of maleimidoethyl 3-(tri-*n*-butylstannyl)hippurate as a radioiodination reagent of antibodies for diagnostic and therapeutic applications. Bioconjugate Chem., *7:* 628–637, 1996.
24. Kenny, A. J., and Maroux, S. Topology of microvillar membrane hydrolases of kidney and intestine. Physiol. Rev., *62:* 91–128, 1982.
25. Arano, Y., Wakisaka, K., Ohmomo, Y., Uezono, T., Mukai, T., Motonari, H., Shiono, H., Sakahara, H., Konishi, J., Tanaka, C., and Yokoyama, A. Maleimidoethyl 3-(tri-*n*-butylstannyl)hippurate: a useful radioiodination reagent for protein radiopharmaceuticals to enhance target selective radioactivity localization. J. Med. Chem., *37:* 2609–2618, 1994.
26. Wakisaka, K., Arano, Y., Uezono, T., Akizawa, H., Ono, M., Kawai, K., Ohmomo, Y., Nakayama, M., and Saji, H. A novel radioiodination reagent for protein radiopharmaceuticals with L-lysine as a plasma-stable metabolizable linkage to liberate *m*-iodohippuric acid after lysosomal proteolysis. J. Med. Chem., *40:* 2643–2652, 1997.
27. Skidgel, R. A. Basic carboxypeptidases: regulators of peptide hormone activity. Trends Pharmacol. Sci., *91:* 299–304, 1988.
28. Arano, Y., Wakisaka, K., Akizawa, H., Ono, M., Kawai, K., Nakayama, M., Sakahara, H., Konishi, J., and Saji, H. Assessment of the radiochemical design of antibodies with a metabolizable linkage for target-selective radioactivity delivery. Bioconjugate Chem., *9:* 497–506, 1998.
29. Hosoi, S., Nakamura, T., Higashi, S., Yamamuro, T., Toyama, S., Shinomiya, K., and Mikawa, H. Detection of human osteosarcoma-associated antigen(s) by monoclonal antibodies. Cancer Res., *42:* 654–659, 1982.
30. Gorevic, P. D., Prelli, F. C., and Frangione, B. Purification and characterization of serum immunoglobulins. Methods Enzymol., *116:* 3–25, 1985.
31. Meares, C. F., McCall, M. J., Reardan, D. T., Goodwin, D. A., Diamanti, C. I., and McTigue, M. Conjugation of antibodies with bifunctional chelating agents: isothiocyanate and bromoacetamide reagents, methods of analysis, and subsequent addition of metal ions. Anal. Biochem., *142:* 68–78, 1984.
32. Grassetti, D. R., and Murray, F. M., Jr. Determination of sulfhydryl groups with 2,2′- or 4,4′-dithiopyridine. Arch. Biochem. Biophys., *119:* 41–49, 1967.
33. Imai, S., Morimoto, J., Tsubura, T., Esaki, K., Michalides, R., Holms, R. S., Deimling, O., and Higlgers, J. Genetic marker patterns and endogenous mammary tumor virus genes in inbred mouse strains in Japan. Exp. Anim., *35:* 263–276, 1986.
34. Arano, Y., Mukai, T., Uezono, T., Wakisaka, K., Motonari, H., Akizawa, H., Taoka, Y., and Yokoyama, A. A biological method to evaluate bifunctional chelating agents to label antibodies with metallic radionuclides. J. Nucl. Med., *35:* 890–898, 1994.
35. Wallner, S. J., and Walker, J. E. Glycosidases in cell wall-degrading extracts of ripening tomato fruits. Plant Physiol., *55:* 93–98, 1975.
36. Razzell, W. E. Phosphodiesterases. Methods Enzymol., *6.* 236–258, 1963.
37. Arano, Y., Matsushima, H., Tagawa, M., Koizumi, M., Endo, K., Konishi, J., and Yokoyama, A. A novel bifunctional metabolizable linker for the conjugation of antibodies with radionuclides. Bioconjugate Chem., *2:* 71–76, 1991.



Downloaded from http://aacrjournals.org/cancerres/article-pdf/59/1/128/3228790/ch0199000128o.pdf by guest on 05 November 2024